Thermal charge carrier driven noise in transmissive semiconductor optics

F. Bruns,[1] S. P. Vyatchanin,[2] J. Dickmann,[3] R. Glaser,[4] D. Heinert,[4] R. Nawrodt,[5] and S. Kroker[3, 1]

[1] *Technische Universität Braunschweig, LENA Laboratory for Emerging Nanometrology,*
Pockelsstraße 14, 38106 Braunschweig, Germany
[2] *Faculty of Physics, M.V. Lomonosov Moscow State University, Moscow 119991, Russia,*
Quantum Technology Centre, M.V. Lomonosov, Moscow State University, Moscow 119991, Russia
[3] *Physikalisch-Technische Bundesanstalt, Bundesallee 100, 38116 Braunschweig, Germany*
[4] *Institut für Festkörperphysik, Friedrich-Schiller-Universität Jena, 07743 Jena, Germany*
[5] *5. Physikalisches Institut, Universität Stuttgart, 70569 Stuttgart, Germany*
(Dated: February 3, 2020)

Several sources of noise limit the sensitivity of current gravitational wave detectors. Currently, dominant noise sources include quantum noise and thermal Brownian noise, but future detectors will also be limited by other thermal noise channels. In this paper we study a thermal noise source which is caused by spatial charge carrier density variations in semiconductor materials. We provide an analytical model for the understanding of charge carrier fluctuations under the presence of screening effects and show that charge carrier noise will not be a limiting noise source for third generation gravitational wave detectors.

I. INTRODUCTION

Gravitational wave detection (GWD) [1, 2] is an exciting and growing field in the realm of high-precision metrology. For the first detection of a gravitational wave, complex infrastructure was built taking huge care to reduce all of the possible noise sources. In particular the fascinating accuracy of a displacement measurement of a macroscopic test mass is demonstrated on a level of about $\sim 10^{-18}$ m [3–8].

A third generation of gravitational wave detectors is planned in order to access gravitational waves as a new channel of information into the universe addressing fundamental questions such as the nature of dark matter, the inner structure of black holes and the origin of the universe itself [9]. For third generation gravitational wave detectors (Einstein Telescope in Europe or Voyager and Cosmic Explorer in USA) the use of crystalline materials is considered [10]. Third generation gravitational wave detectors are severely limited by thermal noise and will therefore be run at cryogenic temperatures. At these temperatures crystalline materials have superior mechanical quality factors compared to conventional amorphous materials thus being less susceptible to thermal Brownian noise [11–16]. Therefore, semiconductors such as galliumarsenide and silicon are considered as suitable substrate materials. This class of materials is potentially susceptible to novel noise channels.

In this paper we study thermal carrier noise in semiconductor materials. Similary to thermochemical noise [17] which is caused by the diffusion of optical impurities this source of noise originates from the thermal motion of free charge carriers in the transmissive optical elements. The Brownian motion of charge carriers leads to spatial variations of the free carrier density thus creating local fluctuations of the refractive index. These fluctuations will be probed by any beam of light transmitted through the optical element. Below we refer to this noise as thermal charge carrier refractive (TCCR) noise. For free charge carriers screening effects have to be considered which distinguishes TCCR noise from thermochemical noise. A quantitative analysis of TCCR noise is presented taking into account Debye screening which depresses TCCR noise.

II. PROBLEM STATEMENT

Earthbound gravitational wave detectors consist of a large scale Michelsen interferometer with Fabry-Perot (FP) cavities in the arms for signal enhancement [18]. An incoming gravitational wave with the strain h displaces the endmirrors of the FP cavities by a length of δl:

$$\delta l = \frac{L_0 h}{2}. \tag{1}$$

In order to measure the variation of the gravitational metric h the displacement of the endmirrors is probed with a laser beam. The displacement of the end mirrors causes a phase shift between the interferometerarms which is enhanced by the FP-cavities and read out via interference of laser light of the two arm cavities.

In this paper we investigate transmissive optics made of semiconductor materials which is particulary important for third generation gravitational wave detectors such as the Einstein telescope. In semiconductor optics such as galliumarsenide or silicon [19] free charge carriers are present. These charge carriers move thermally akin to Brownian motion thus creating local charge carrier density fluctuations η. As stated by Soref *et al.* [20] the refractive index n is dependent on the charge carrier concentration as an effect of the free carrier dispersion:

$$\delta n = \beta \eta, \quad \beta = \frac{-e^2}{2\epsilon_0 n \omega_l^2 m_e}, \tag{2}$$

with ω_l the laser frequency, n the refractive index of the semiconductor, e the elementary charge and m_e the

effective electron mass. That is why the local charge carrier fluctuations η cause fluctuations of the refractive index δn. These fluctuations are probed by any laser beam propagating through the optical element.

When a Gaussian laser beam propagates a distance L along the z-axis inside of e.g. the input mirror (test mass) of a FP cavity (see Fig. 1), it reads out the information on the variation of the refractive index inside the input test mass weighted by the light intensity distribution in the cross section. Hence, the optical path length of the laser beam is shifted by a value of ξ:

$$\xi(t) = \beta \int \eta(\vec{r}, t) \cdot \Psi(\vec{r}) \, d\vec{r}, \tag{3}$$

$$\Psi(\vec{r}) = \begin{cases} \frac{e^{-(x^2+y^2)/r_0^2}}{\pi r_0^2}, & \text{if } |z| \leq \frac{L}{2} \\ 0, & \text{if } |z| > \frac{L}{2} \end{cases}, \tag{4}$$

where L is the length of the mirror substrate, r_0 is the Gaussian radius of the light beam (referring to the length where the amplitude falls off by e^{-1}), x, y are the transversal coordinates and $\int d\vec{r}$ is an integration over the volume of the input test mass. In the measurement we cannot distinguish between a fluctuation of the optical path length caused by noise or a length shift of the mirror caused by a gravitational wave. In this way carrier density fluctuations η inside transmissive semiconductor optics contribute to the measured strain as h_ξ:

$$\eta \to \xi \to h_\xi.$$

We call this noise thermal charge carrier refractive (TCCR) noise. In order to quantify TCCR noise we have to model the carrier density fluctuations under consideration of screening effects that occur for free charge carriers (section II B). Furthermore we have to understand how a change in the optical path length ξ is related to the strain h caused by the gravitational wave (section II A) and combine both to get an expression for the amplitude of TCCR noise (section II C). Finally we use this to explicitly compute the TCCR noise of ET input test masses (section III).

A. Coupling of noise induced changes in the path length and the measured strain

For simplicity reasons we consider a Michelson configuration with interferometer arms perpendicular to each other. To establish our model for TCCR noise we examine a Fabry-Perot (FP) cavity with mirrors as free test masses as shown in Fig. 1. TCCR noise in the input test mass disturbs the optical path length nL by a value of ξ. From input-output relations we can see that the reflected amplitude B (see notations on Fig. 1) contains an additional fluctuation term in the frequency domain:

$$b_\xi = \frac{\gamma + i\Omega}{\gamma - i\Omega} \cdot Aik\xi + Aik\xi = Aik\xi \cdot \frac{2\gamma}{\gamma - i\Omega}, \tag{5}$$
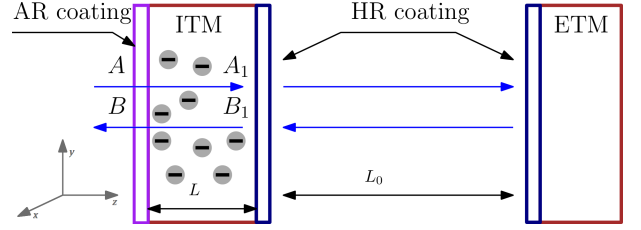

Figure 1: Fabry-Perot cavity. The surfaces of the input test mass are covered by anti-reflecting (AR) and high reflecting (HR) coatings. The thermal motion of carriers in the input test mass produces additional fluctuations of the refractive index wich are probed by the transmitted beams. The position of the coordinate system has been been shifted for better visibility. Its center is actually at the center of mass of the input mirror.

where Ω is a spectral frequency, $\gamma = T^2/2\tau$ is the amplitude relaxation rate of the FP cavity, $\tau = 2L_0/c$ is the round trip time (usually $\Omega\tau \ll 1$) and T and R are the amplitude transmittance and reflectance of the input test masses ($R^2 + T^2 = 1$, we assume $T \ll 1$). The two terms in the first equation of (5) describe the perturbation created in the incident wave (after circulation inside the cavity) and the directly reflected one respectively. Effectively the cavity acts as a through pass Lorentz filter.

The fluctuation term should be compared with the signal term b_s produced by the displacement $\delta L = L_0 h_s/2$ (h_s is the perturbation of the metric caused by the gravitational wave):

$$b_s = T \cdot \frac{2A}{T} \cdot \frac{2ik\,\delta L}{1 - Re^{i\Omega\tau}} = \frac{2A \cdot ikL_0}{\tau(\gamma - i\Omega)} \cdot h_s. \tag{6}$$

For LIGO Voyager or the ET interferometer there are FP cavities in east and north arms, the light from them interfere on a 50/50 beam splitter. Thus, the signal b_s (6) of the gravitational wave is increased by a factor of $\sqrt{2}$:

$$b_s^{\text{ET}} \implies b_s\sqrt{2}. \tag{7}$$

On the other hand there are fluctuations ξ_n and ξ_e in the input test masses of the north and east arm cavities. As follows:

$$b_\xi^{\text{ET}} = Aik \cdot \frac{2\gamma}{\gamma - i\Omega} \cdot \xi_{\text{ET}}, \quad \xi_{\text{ET}} = \frac{\xi_e + \xi_n}{\sqrt{2}}. \tag{8}$$

Note that the fluctuations ξ_e and ξ_n do not depend on each other and have equal power spectral densities. The power spectral density of ξ_{ET} is equal to the power spectral density of ξ_e (or ξ_n). Comparing (5) and (6) by taking into account (7) and (8) one can find that the variation of the gravitational metric h and the optical path fluctuations ξ are related as:

$$h = h_s + h_\xi, \quad h_\xi = \frac{\gamma\tau}{\sqrt{2}} \cdot \frac{\xi_{\text{ET}}}{L_0} = \frac{\pi}{\sqrt{2}\,F} \cdot \frac{\xi_{\text{ET}}}{L_0}, \tag{9}$$

with F the Finesse of the Fabry-Perot cavity.

B. Thermal charge carrier density fluctuations

As suggested by the fluctuation-dissipation theorem we have to understand the dissipation mechanism (in our case that is diffusion) to describe fluctuations of charge carriers. For this reason we derive a diffusion equation including screening effects. We expect Debye screening to suppress diffusion processes thus reducing the fluctuations in the optical elements. Because of the residual doping in the large test mass substrates required for GW detection a majority charge carrier is present [21]. Without loss of generality we assume electrons to be the majority charge carriers. We start with the continuity equation for the carrier concentration n_{cc} [22]:

$$\frac{\partial n_{cc}}{\partial t} = -\vec{\nabla} \cdot \vec{J},$$

(10)

where $\vec{J}$ is the current density described by [22]:

$$\vec{J} = -D\vec{\nabla} n_{cc} + n_{cc}\mu \vec{E},$$

(11)

$$\mu = \frac{eD}{k_B T}.$$

(12)

Here D is the diffusion coefficient, μ the carrier mobility, e the carrier charge, k_B is the Boltzmann constant and T the temperature. The last term in (11), which is proportional to a small electric field $\vec{E}$, is introduced to account for Debye screening. The carrier concentration n_{cc} can be described as a sum of a large constant n_0 and a small fluctuating part η:

$$n_{cc} = n_0 + \eta, \quad n_0 = \frac{1}{e\mu\rho_e},$$

(13)

with the electrical resistivity ρ_e. The screening electric field $\vec{E}$ is given by the Poisson equation [22]:

$$\vec{\nabla} \cdot \vec{E} = \frac{en_{cc}}{\epsilon\epsilon_0} \simeq \frac{e\eta}{\epsilon\epsilon_0}.$$

(14)

Here $\epsilon = n^2$ is the dielectric constant and ϵ_0 the vacuum permittivity. After substituting (11) into (10) whilst using (13) we get:

$$\frac{\partial \eta}{\partial t} = D\Delta\eta - n_0\mu\vec{\nabla}\vec{E}.$$

(15)

Since η is a small deviation from thermal equilibrium (i.e. a fluctuation) we have neglected any quadratic term of η. Finally we get a diffusion equation utilizing (14):

$$\frac{\partial \eta}{\partial t} = D\left(\Delta\eta - \frac{1}{\ell_D^2}\eta\right), \quad \ell_D = \sqrt{\frac{\epsilon\epsilon_0 k_B T}{n_0 e^2}}.$$

(16)

Here $\Delta = (\vec{\nabla})^2$ is the Laplace operator and ℓ_D is the Debye length. Compared to conventional diffusion equations there is an additional term, $-D\,\eta/\ell_D^2$, which is a direct consequence of screening effects under the assumption of only having small deviations from thermal equilibrium η.

Next we want to include fluctuations. In the frame of Langevin approach [23, 24] we introduce the Langevin forces $F(\vec{r}, t)$ into the right part of (16):

$$\frac{\partial \eta}{\partial t} = D\left(\Delta\eta - \frac{1}{\ell_D^2}\eta\right) + F(\vec{r}, t).$$

(17)

These Langevin forces $F(\vec{r}, t)$ cause the Brownian movement of the charge carriers. They are uncorrelated representing white Gaussian noise:

$$\langle F(\vec{k}, \omega)F^*(\vec{k}', \omega')\rangle = (2\pi)^4 F_0^2 \left(k^2 + \ell_D^{-2}\right) \times (\delta(\vec{k} - \vec{k}')\,\delta(\omega - \omega')).$$

(18)

The correlators of the fluctuation forces and the constant F_0 should be chosen to fulfil the equation:

$$\langle \eta^2 \rangle = \frac{n_0}{V},$$

(19)

which corresponds to the well known requirement (of a Poisson process) that the variation $\langle \Delta N^2 \rangle$ of the particle number in a volume V is equal to the mean particle number: $\langle \Delta N^2 \rangle = \langle N \rangle$ [25]. From (19) one can find:

$$F_0^2 = 2Dn_0.$$

(20)

Now we can calculate the auto-correlation function of density fluctuations:

$$B(\vec{\rho}, \tau) \equiv \langle \eta(\vec{r}, t)\eta(\vec{r} - \vec{\rho}, t - \tau)\rangle =$$
$$= \frac{2Dn_0}{(2\pi)^4} \int d\vec{k}\, d\omega\, \frac{\left(k^2 + \frac{1}{\ell_D^2}\right) e^{i\omega\tau + i\vec{k}\vec{\rho}}}{D^2\left(k^2 + \frac{1}{\ell_D^2}\right)^2 + \omega^2}.$$

(21)

From that the *double-sided* power spectral density (PSD) $S_{\eta,\eta}(\vec{k}, \omega)$ can be found using the Wiener-Khinchin theorem [26]:

$$S_{\eta\eta}(\vec{k}, \omega) = \int B(\vec{\rho}, \tau)\, e^{-i\omega\tau - i\vec{k}\vec{\rho}}\, d\vec{\rho}\, d\tau =$$
$$= n_0 \cdot \frac{2D\left(k^2 + \frac{1}{\ell_D^2}\right)}{D^2\left(k^2 + \frac{1}{\ell_D^2}\right)^2 + \omega^2}.$$

(22)

C. Variations of the optical path length

Now that we know the spectral noise density of charge carrier fluctuation (22) and how a shift of the optical change of path length relates to the gravitational strain (9) we can combine these two results with the readout of the Gaussian beam (3) to get the measurable TCCR noise in a gravitational wave detector. The readout of the Gaussian beam, equation (3), can be rewritten as:

$$\xi(t) = \beta \int \frac{d\vec{k}\, d\omega}{(2\pi)^4}\, \eta(\vec{k}, \omega)\, \Psi(\vec{k})\, e^{i\omega t},$$

(23)

where $\eta(\vec{k}, \omega)$ and $\Psi(\vec{k})$ are Fourier transforms of $\eta(\vec{r}, t)$ and $\Psi(\vec{r})$ respectively. To get the PSD of ξ we calculate the auto-correlation function of ξ:

$$\langle \xi(t)\, \xi(t-\tau) \rangle = \beta^2 \int \frac{d\vec{k}\, d\omega}{(2\pi)^4} \frac{d\vec{k}'\, d\omega'}{(2\pi)^4} \tag{24}$$

$$\times \left\langle \eta(\vec{k}, \omega)\, \eta^*(\vec{k}', \omega') \right\rangle \Psi(\vec{k})\, \Psi^*(\vec{k}')\, e^{i\omega t - i\omega'(t-\tau)}.$$

Using (18) we can express the correlator as:

$$\langle \eta(\vec{k}, \omega)\, \eta^*(\vec{k}', \omega') \rangle = \frac{\left(k^2 + \frac{1}{\ell_D^2} \right)}{\omega^2 + D^2 \left(k^2 + \frac{1}{\ell_D^2} \right)^2}$$

$$\times (2\pi)^4\, F_0^2 \cdot \delta(\vec{k} - \vec{k}')\, \delta(\omega - \omega'), \tag{25}$$

and substituting into (24) and using the Wiener-Khinchin theorem and the normalisation (20) we write down the double-sided PSD $S_{\xi\xi}(\omega)$:

$$S_{\xi\xi}(\omega) = 2Dn_0\beta^2 \int \frac{d\vec{k}}{(2\pi)^3} \cdot \frac{\left(k^2 + \frac{1}{\ell_D^2} \right) |\Psi(\vec{k})|^2}{\omega^2 + D^2 \left(k^2 + \frac{1}{\ell_D^2} \right)^2}. \tag{26}$$

With the results of section II A we can rewrite (26) in terms of the GW metric using (9):

$$S_{\xi\xi}^h(\omega) = \frac{n_0\beta^2(\gamma\tau)^2}{L_0^2} \int \frac{d\vec{k}}{(2\pi)^3} \cdot \frac{D\left(k^2 + \frac{1}{\ell_D^2} \right) |\Psi(\vec{k})|^2}{\omega^2 + D^2 \left(k^2 + \frac{1}{\ell_D^2} \right)^2}. \tag{27}$$

In the usual case, when the Debye length is much smaller than the physical dimensions of the systems, i.e. the Gaussian radius and the length of the substrate (see table II), $\ell_D \ll r_0, L$ this expression can be simplified:

$$S_{\xi\xi}^h(\omega) = \frac{n_0\beta^2(\gamma\tau)^2}{L_0^2} \cdot \frac{L}{2\pi r_0^2} \cdot \frac{\tau}{1 + \omega^2\tau^2}, \tag{28}$$

$$\tau = \frac{\ell_D^2}{D} = \epsilon\epsilon_0\rho, \tag{29}$$

where τ is the Maxwell relaxation time. Here we used the normalisation:

$$\int \frac{d\vec{k}}{(2\pi)^3} |\Psi(\vec{k})|^2 = \int d\vec{r} |\Psi(\vec{r})|^2 = \frac{L}{2\pi r_0^2}. \tag{30}$$

The PSD can be converted into the amplitude spectral density (ASD):

$$S_{\xi}^h(\omega) = \sqrt{S_{\xi\xi}^h(\omega)}. \tag{31}$$

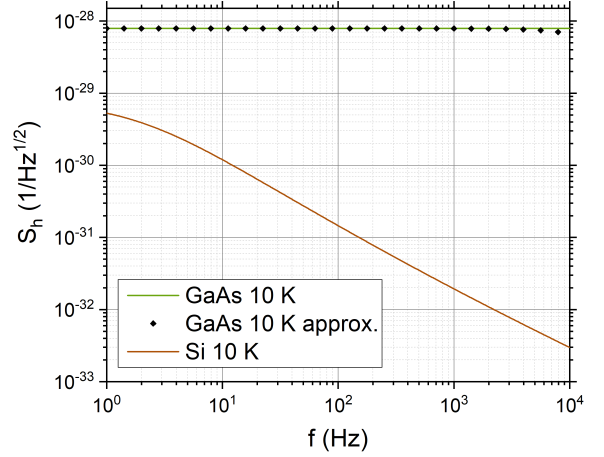Note that formula (27) for the spectral noise density is valid for frequencies smaller than the inverse diffusion

Figure 2: ASD of TCCR noise in the input test mass substrates of ET at 10 K for pure Si, $n_D = 5 \cdot 10^{12}\, \frac{1}{cm^3}$, and lowly doped GaAs, $n_D = 5 \cdot 10^{13}\, \frac{1}{cm^3}$. The approximated formula (28) is valid for lowly doped GaAs at 10 K but cannot be used for pure Si at 10 K because of the more pronounced freeze out of charge carriers in an indirect semiconductor such as Si enabling the Debye length to become of order of the Gaussian beam radius (see table II). At small Debye lengths and small frequencies the ASD of TCCR noise is independent of frequency as can be seen for GaAs.

time because the equation of motion (15) does not account for retardation effects. The diffusion time is either determined by the Maxwell rexalation time or the electron lifetime whatever is smaller [27]. In silicon (Si) which is an indirect semiconductor the diffusion time is given by the Maxwell relaxation time (29) which is around 10^{-8} s for pure Si at room temperature whereas in galliumarsenid (GaAs) as a direct semiconductor the diffusion time is given by the electron lifetime of about 10^{-9} s [28]. The limiting frequencies are therefore around 10^8 Hz and 10^9 Hz which is much larger than the frequency range of third generation gravitational wave detectors of 1 to 10^4 Hz [19].

III. COMPUTATION OF TCCR NOISE

To quantify the magnitude of TCCR noise we are going to focus on the third generation gravitational wave detector the Einstein telescope where the use of crystalline substrate materials is considered. The HR and AR coatings do not contribute to TCCR noise significantly because they are amorphous thus having much less free charge carriers.

TCCR noise is dependent on the diffusion coefficient D and the Debye length ℓ_D (see table II for numerical values of D and ℓ_D). This is why it is indirectly also a function of temperature T and doping density n_D. At this time large high-purity silicon samples can be produced with
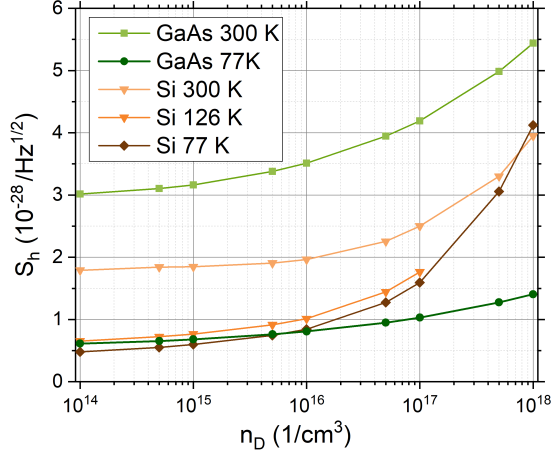
Figure 3: Doping dependency of the ASD of TCCR noise S_h^ξ. At the shown temperatures the ASD is a constant of frequency in the frequency interval of 1 to 10^4 Hz for both GaAs and Si. Due to a lack of data for the charge carrier mobility μ of doped materials at cryogenic temperatures we show the temperatures 77 K, 126 K and 300 K. The temperature of 126 K is interesting because at this temperature the thermoelastic coefficient vanishes immensely reducing the thermoelastic noise. The ASD of Si at 77 K and Si at 300 K cross due to a crossing of the charge carrier mobility at high levels of doping (see table II).

Table I: Parameters of the input test masses of the Einstein telescope [19, p.347].

parameter	symbol	value
finesse of FP cavity	F	880
mirror thickness	L	0.5 m
Gaussian radius	r_0	0.09 m
laser wavelength	λ_L	1550 nm
arm length	L_0	10^4 m
refractive index Si [29]	n	3.487
refractive index GaAs [30]	n	3.370
effective electron mass Si	m_e	0.260 m_0
effective electron mass GaAs	m_e	0.063 m_0
electron rest mass	m_0	$9.109 \cdot 10^{-31}$ kg
Boltzmann constant	k_B	$1.380 \cdot 10^{-23}$ $\frac{J}{K}$
vaccum permittivity	ϵ_0	$8.854 \cdot 10^{-12}$ $\frac{As}{Vm}$

the magnetically assisted Czochralski technique with a resistivity of up to 10 kΩcm. To account for difficulties we are looking at n-type silicon with a worse resistivity of 1 kΩcm which corresponds to a doping density of around $4.4 \cdot 10^{12}$ $\frac{1}{cm^3}$, which is equivalent to a resistivity of $1\,k\Omega cm$ at room temperature [21]. In order to calculate the mean carrier density n_0 as a function of the doping density a model for semiconductors with no

compensation (no acceptors) has been used [31]:

$$n_0 = \frac{2n_D}{1 + \left[1 + 4g_D \frac{n_D}{n_c} \exp\left(\frac{E_D^b}{k_B T}\right)\right]^{1/2}}. \quad (32)$$

Here g_D is the donor degeneracy, n_D is the donor concentration, E_D^b is the energy gap between donor level and the conduction band and n_c is the conduction band edge density:

$$n_c = 2 \left(\frac{m_{e,b}^* k_B T}{2\pi \hbar^2}\right)^{3/2}, \quad (33)$$

with $m_{d,e}^*$ the effective density of states mass of the conduction band electrons. As dopants we considered shallow phosphorous donors which have a degeneracy of $g_D = 2$ and an energy gap of $E_D^b = 45$ meV.

Additionally, we want to be able to model the diffusion coefficient D. For this we used the Einstein-Smoluchowski equation in order to replace the diffusion coefficient D with the well investigated charge carrier mobility μ [31]:

$$D = \frac{k_B T}{e}\mu. \quad (34)$$

A more precise expression for D can be obtained from taking into account the carrier band curvature. In our case though, the Fermi level is several eV deep within the band gap. Thus, the deviations from the Einstein-Smoluchowski equation are negligibly small. The mobility data for modeling D has been obtained from Jacoboni et al. [32], Li et al. [33], Sotoodeh et al. [34] and Wolfe et al. [35].

In Fig. 2 we have plotted the ASD of TCCR noise of the ET input test masses at its operation temperature of 10 K for pure Si, $n_D \approx 5 \cdot 10^{12}$ $\frac{1}{cm^3}$, and weakly doped GaAs, $n_D \approx 5 \cdot 10^{13}$ $\frac{1}{cm^3}$, using the parameters shown in table I and II. All numerical calculations shown have been performed with Mathematica 11.3 [36].

We can see that the ASD of TCCR noise at 10 K reaches $7.9 \cdot 10^{-29}$ $/\sqrt{Hz}$ in GaAs and $5.3 \cdot 10^{-30}$ $/\sqrt{Hz}$ in Si. These noise amplitudes are well below the sensitivity goal of the ET telescope of $3 \cdot 10^{-25}$ $\sqrt{Hz}$. Therefore we can come to the important conclusion that TCCR noise is not a limiting noise source for the ET telescope and third generation GWD in general.

Interestingly, the frequency dependencies of GaAs and Si at 10 K is vastly different (see Fig. 2). We can see that the ASD of Si falls off with f^{-1} as is typical for Brownian noise sources. On the other hand the ASD of GaAs is a constant in the shown frequency interval. The frequency behaviour of TCCR noise is dependent on the Debye length. Going back to formula (28) we can see that for small Debye lengths ℓ_D the denominator can be approximated thus obtaining a frequency independent PSD. Si is an indirect semiconductor in contrast to GaAs. Therefore, its free charge carriers freeze out more quickly

than in a direct semiconductor like GaAs. This increases the Debye length (see (16)). For this reason the Debye length of Si is much larger than GaAs at 10 K (compare table II). This explains their difference in frequency behaviours. At higher temperatures (larger than 70 K) a plateau of constant TCCR noise up to at least 10^4 Hz can be found for both semiconductors.

Like all thermal noise sources TCCR noise scales with temperature, additionally it also increases with the doping concentration. In Fig. 3 we are showing the ASD of TCCR noise in dependence of the doping density for different temperatures. The doping dependence can be explained in the following way: An increasing doping density n_D generally decreases the charge carrier mobility μ and the diffusion coefficient D respectively (see table II) thus increasing the TCCR noise amplitude. Also with increasing levels of doping the mean carrier density n_0 increases thus reducing the Debye length ℓ_D. Both n_0 and ℓ_D affect the TCCR noise amplitude but these effects compensate each other completely as can be seen in (28). Overall we can come to the conclusion that even for room temperatures (compared to cryogenic operation) and high doping densities TCCR noise stays below the sensitivity targets of third generation wave detectors.

IV. CONCLUSION

We show a detailed analysis of thermal charge carrier refractive (TCCR) noise in metals and semiconductors from first principles especially taking into account screening effects. We show that Debye screening practically blocks diffusion processes, hence dramatically reducing TCCR noise. We apply our approach to the input masses of the Einstein telescope and show that TCCR noise is not limiting a limiting noise source. Furthermore it can be seen that TCCR noise does not increase significantly at room temperature (compared to cryogenic operation) and high levels of doping of the material. For instance for the input test masses of ET at room temperature and a rather high doping density of $n_D = 10^{16} \frac{1}{cm^3}$ the TCCR noise amplitude is three orders of magnitude below the design sensitivity. Before this paper the driver for ultra-pure silicon has been optical absorption and TCCR noise. With our derivation we show that TCCR noise is not a limiting noise source for substrate materials of third generation gravitational wave detectors. Nevertheless there is still a need for ultra-pure substrate materials due to limits set by the optical absorption [37] [21].

[1] B. P. Abbott *et al.* Observation of Gravitational Waves from a Binary Black Hole Merger. *Phys. Rev. Lett.*, 116:061102, Feb 2016.

[2] B. P. Abbott *et al*, (LIGO Scientific Collaboration and Virgo Collaboration). GW151226: Observation of Gravitational Waves from a 22-Solar-Mass Binary Black Hole Coalescence. *Phys. Rev. Lett.*, 116:241103, 2016.

[3] LVC-Collaboration. Prospects for Observing and Localizing Gravitational-Wave Transients with Advanced LIGO and Advanced Virgo. *arXiv*, 1304.0670, 2013.

[4] K.L. Dooley, T. Akutsu, S. Dwyer, and P. Puppo. Status of advanced ground-based laser interferometers for gravitational-wave detection. *arXiv*, 1411.6068, 2014.

[5] J. Aasi, B.P. Abbott, et al. Advanced LIGO. *Classical and Quantum Gravity*, 32:074001, 2015.

[6] J. Abadie and et. al. Advanced LIGO. *Classical and Quantum Gravity*, 32:074001, 2015.

[7] F. Acernese et al, (Virgo Collaboration). Advanced Virgo: a 2nd generation interferometric gravitational wave detector. *Classiacal and Quantum Gravity*, 32:024001, 2015.

[8] F. Acernese et al (Virgo Collaboration). Calibration of Advanced Virgo and Reconstruction of the Gravitational Wave Signal h(t) during the Observing Run O2. *arXiv*, 1807.03275, 2018.

[9] B Sathyaprakash. Corrigendum: Scientific objectives of einstein telescope. *Classical and Quantum Gravity*, 30(7):079501, mar 2013.

[10] S. Wills. Gravitational WavesThe Road Ahead . *Optics and Photonics News*, page 44–52, May 2018.

[11] R. Nawrodt, S. Rowan, J. Hough, M. Punturo, F. Ricci, and J.-Y. Vinet. Challenges in thermal noise for 3rd generation of gravitational wave detectors. *Gen. Relativ. Grav.*, 43:593–622, 2011.

[12] I W Martin et al. Effect of heat treatment on mechanical dissipation in ta2o5 coatings. *Classical and Quantum Gravity*, 27(22):225020, oct 2010.

[13] I. Martin et al. Measurements of a low-temperature mechanical dissipation peak in a single layer of Ta_2O_5 doped with TiO_2. *Class. Quantum Grav.*, 25:055005, 2008.

[14] R. Nawrodt, A. Zimmer, T. Koettig, C. Schwarz, D. Heinert, M. Hudl, R. Neubert, M. Thürk, S. Nietzsche, W. Vodel, and P. Seidel. High mechanical Q-factor measurements on silicon bulk samples. *J. Phys.: Conf. Ser.*, 122:012008, 2008.

[15] I W Martin, R Nawrodt, K Craig, C Schwarz, R Bassiri, G Harry, J Hough, S Penn, S Reid, R Robie, and S Rowan. Low temperature mechanical dissipation of an ion-beam sputtered silica film. *Classical and Quantum Gravity*, 31(3):035019, jan 2014.

[16] R. Nawrodt et al. High mechanical q-factor measurements on calcium fluoride at cryogenic temperatures. *The European Physical Journal - Applied Physics*, 38(1):53–59, 2007.

Table II: Electron mobility μ, diffusion coefficient D and Debye length ℓ_D of GaAs and Si at different temperatures. The mobility data of Si at 126 K has been approximated by taking the mean of the mobilities at 100 K and 150 K from Li *et al* [33].

		Silicon			GaAs		
T[K]	n_D [1/cm³]	μ [m²/Vs]	D [m²/s]	ℓ_D [m]	μ [m²/Vs]	D [m²/s]	
10	$5 \cdot 10^{12}$	38.8 [32]	$3.34 \cdot 10^{-2}$	$9.38 \cdot 10^{-2}$	-	-	-
10	$5 \cdot 10^{13}$	-	-	-	12.8 [35]	$1.10 \cdot 10^{-2}$	$1.06 \cdot 10^{-6}$
77	10^{14}	2.04 [33]	$1.35 \cdot 10^{-2}$	$6.84 \cdot 10^{-7}$	21.1 [35]	$1.40 \cdot 10^{-1}$	$2.96 \cdot 10^{-7}$
77	$5 \cdot 10^{14}$	1.55 [33]	$1.03 \cdot 10^{-2}$	$4.51 \cdot 10^{-7}$	18.6 [35]	$1.23 \cdot 10^{-1}$	$1.82 \cdot 10^{-7}$
77	10^{15}	1.31 [33]	$8.67 \cdot 10^{-3}$	$3.78 \cdot 10^{-7}$	17.2 [35]	$1.14 \cdot 10^{-1}$	$1.49 \cdot 10^{-7}$
77	$5 \cdot 10^{15}$	0.845 [33]	$5.61 \cdot 10^{-3}$	$2.52 \cdot 10^{-7}$	13.7 [35]	$9.06 \cdot 10^{-2}$	$9.71 \cdot 10^{-8}$
77	10^{16}	0.655 [33]	$4.35 \cdot 10^{-3}$	$2.12 \cdot 10^{-7}$	12.2 [35]	$8.08 \cdot 10^{-2}$	$8.11 \cdot 10^{-8}$
77	$5 \cdot 10^{16}$	0.287 [33]	$1.90 \cdot 10^{-3}$	$1.41 \cdot 10^{-7}$	8.81 [35]	$5.85 \cdot 10^{-2}$	$5.38 \cdot 10^{-8}$
77	10^{17}	0.184 [33]	$1.22 \cdot 10^{-3}$	$1.19 \cdot 10^{-7}$	7.48 [35]	$4.96 \cdot 10^{-2}$	$4.51 \cdot 10^{-8}$
77	$5 \cdot 10^{17}$	0.050 [33]	$3.32 \cdot 10^{-4}$	$7.94 \cdot 10^{-8}$	4.88 [35]	$3.24 \cdot 10^{-2}$	$3.01 \cdot 10^{-8}$
77	10^{18}	0.027 [33]	$1.82 \cdot 10^{-4}$	$6.67 \cdot 10^{-8}$	4.02 [35]	$2.66 \cdot 10^{-2}$	$2.53 \cdot 10^{-8}$
126	10^{14}	1.09	$1.19 \cdot 10^{-2}$	$4.19 \cdot 10^{-7}$	-	-	-
126	$5 \cdot 10^{14}$	0.895	$9.72 \cdot 10^{-3}$	$2.61 \cdot 10^{-7}$	-	-	-
126	10^{15}	0.795	$8.63 \cdot 10^{-3}$	$2.15 \cdot 10^{-7}$	-	-	-
126	$5 \cdot 10^{15}$	0.557	$6.05 \cdot 10^{-3}$	$1.41 \cdot 10^{-7}$	-	-	-
126	10^{16}	0.456	$4.95 \cdot 10^{-3}$	$1.18 \cdot 10^{-7}$	-	-	-
126	$5 \cdot 10^{16}$	0.224	$2.43 \cdot 10^{-3}$	$7.81 \cdot 10^{-8}$	-	-	-
126	10^{17}	0.150	$1.63 \cdot 10^{-3}$	$6.55 \cdot 10^{-8}$	-	-	-
300	10^{14}	0.146 [33]	$3.76 \cdot 10^{-3}$	$4.33 \cdot 10^{-7}$	0.873 [34]	$2.26 \cdot 10^{-2}$	$4.29 \cdot 10^{-7}$
300	$5 \cdot 10^{14}$	0.138 [33]	$3.56 \cdot 10^{-3}$	$2.14 \cdot 10^{-7}$	0.824 [34]	$2.13 \cdot 10^{-2}$	$2.22 \cdot 10^{-7}$
300	10^{15}	0.137 [33]	$3.54 \cdot 10^{-3}$	$1.64 \cdot 10^{-7}$	0.795 [34]	$2.05 \cdot 10^{-2}$	$1.73 \cdot 10^{-7}$
300	$5 \cdot 10^{15}$	0.129 [33]	$3.32 \cdot 10^{-3}$	$9.52 \cdot 10^{-8}$	0.696 [34]	$1.80 \cdot 10^{-2}$	$1.04 \cdot 10^{-7}$
300	10^{16}	0.121 [33]	$3.13 \cdot 10^{-3}$	$7.73 \cdot 10^{-8}$	0.644 [34]	$1.67 \cdot 10^{-2}$	$8.52 \cdot 10^{-8}$
300	$5 \cdot 10^{16}$	0.092 [33]	$2.38 \cdot 10^{-3}$	$4.93 \cdot 10^{-8}$	0.510 [34]	$1.32 \cdot 10^{-2}$	$5.50 \cdot 10^{-8}$
300	10^{17}	0.075 [33]	$1.93 \cdot 10^{-3}$	$4.10 \cdot 10^{-8}$	0.452 [34]	$1.17 \cdot 10^{-2}$	$4.59 \cdot 10^{-8}$
300	$5 \cdot 10^{17}$	0.043 [33]	$1.11 \cdot 10^{-3}$	$2.70 \cdot 10^{-8}$	0.320 [34]	$8.26 \cdot 10^{-3}$	$3.03 \cdot 10^{-8}$
300	10^{18}	0.030 [33]	$7.74 \cdot 10^{-4}$	$2.26 \cdot 10^{-8}$	0.268 [34]	$6.93 \cdot 10^{-3}$	$2.54 \cdot 10^{-8}$

[17] Bruin Benthem and Yuri Levin. Thermorefractive and thermochemical noise in the beamsplitter of the geo600 gravitational-wave interferometer. *Phys. Rev. D*, 80:062004, Sep 2009.

[18] P. R. Saulson. *Fundamentals of Interferometric Gravitational Wave Detectors*. World Scientific, Singapore, 1994.

[19] M. Abernathy et al. ET conceptual design study document. 2011.

[20] R. A. Soref and B. R. Bennett. Electrooptical Effects in Silicon. *IEEE Journal of Quantum Electronics*, QE-23:123–129, 1987.

[21] J Degallaix et al. Measurement of the optical absorption of bulk silicon at cryogenic temperature and the implication for the Einstein Telescope. *Classical and Quantum Gravity*, 31(18):185010, aug 2014.

[22] JD Jackson. *Klassische Elektrodynamik*. De Gruyter, 1998.

[23] K. M. van Vliet, A. van der Ziel, and R. R. Schmidt. Temperature-fluctuation noise of thin films supported by a substrate. *J. Appl. Phys.*, 51(6):2947, 1980.

[24] V. B. Braginsky, M. L. Gorodetsky, and S. P. Vyatchanin. Thermodynamical fluctuations and photo-thermal shot noise in gravitational wave antennae. *Phys. Lett. A*, 264:1–10, 1999.

[25] L.L. Landau and E.M. Lifshitz. *Theoretical Physics: Statistical Physics*. vol.5. Butterworth-Heinemann, 1980.

[26] A Chintchin. Korrelationstheorie der stationären stochastischen prozesse. *Mathematische Annalen*, 109, 1934.

[27] D Forster. *Hydrodynamic Fluctuations, Broken Symmetry, and Correlation Functions*. CRC Press, 1975.

[28] Recombination at semiconductor surfaces and interfaces. *Surface Science*, 132(1):406 – 421, 1983.

[29] C. Schinke et al. Uncertainty analysis for the coefficient of band-to-band absorption of crystalline silicon. *AIP Advances*, 5(6):67168, 2015.

[30] T. Skauli et al. Improved dispersion relations for GaAs and applications to nonlinear optics. *J. Appl. Phys.*, 94(10):6447–6455, 2003.

[31] M Grundmann. *The Physics of semiconductors*. Springer, 2016.

[32] C Jacoboni et al. A review of some charge transport properties of silicon. *Solid State Electronics*, 20:77–89, February 1977.

[33] Sheng S. Li and W. Robert Thurber. The dopant density and temperature dependence of electron mobility and resistivity in n-type silicon. *Solid-State Electronics*, 20(7):609–616, 1977.

[34] M. Sotoodeh, A. H. Khalid, and A. A. Rezazadeh. Empirical low-field mobility model for III–V compounds ap-

plicable in device simulation codes. *Journal of Applied Physics*, 87(6):2890–2900, 2000.

[35] C. M. Wolfe, G. E. Stillman, and W. T. Lindley. Electron Mobility in High-Purity GaAs. *Journal of Applied Physics*, 41(7):3088–3091, 1970.

[36] Wolfram Research, Inc. Mathematica, Version 11.3.

[37] W. Winkler, K. Danzmann, A. Rüdiger, and R. Schilling. Heating by optical absorption and the performance of interferometric gravitational-wave detectors. *Phys. Rev. A*, 44:7022–7036, Dec 1991.